# Physical Mechanisms for the Association of El Niño and West African Rainfall with Atlantic Major Hurricane Activity

STANLEY B. GOLDENBERG AND LLOYD J. SHAPIRO

*Hurricane Research Division/AOML, Miami, Florida*

(Manuscript received 14 July 1994, in final form 20 June 1995)

ABSTRACT

Physical mechanisms responsible for the contemporaneous association, shown in earlier studies, of North Atlantic basin major hurricane (MH) activity with western Sahelian monsoon rainfall and an equatorial eastern Pacific sea surface temperature index of El Niño are examined, using correlations with 200- and 700-mb level wind data for the period 1968–92. The use of partial correlations isolates some of the relationships associated with the various parameters.

The results support previous suggestions that the upper- and lower-level winds over the region in the basin between ~10° and 20°N where most MHs begin developing are critical determinants of the MH activity in each hurricane season. In particular, interannual fluctuations in the winds that produce changes in the magnitude of vertical shear are one of the most important factors, with reduced shear being associated with increased activity and stronger shear with decreased activity. The results show that most of these critical wind fluctuations are explained by their relationship to the SST and rainfall fluctuations. Results confirm previous findings that positive (warm) eastern Pacific SST and negative (drought) Sahelian rainfall anomalies are associated with suppressed Atlantic basin tropical cyclone activity through an equatorially confined near-zonal circulation with upper-level westerlies and lower-level easterlies that act to increase the climatological westerly vertical shear in the main development region. SST and rainfall anomalies of the opposite sense are related to MH activity through a zonal circulation with upper-level easterly and lower-level westerly wind anomalies that act to cancel out some of the climatological westerly vertical shear. The results also show that changes in vertical shear to the north of the main development region are unrelated to, or possibly even out of phase with, changes in the development region, providing a possible physical explanation for the observations from recent studies of the out-of-phase relationship of interannual fluctuations in MH activity in the region poleward of ~25°N with fluctuations in activity to the south.

The interannual variability of MH activity explained by Sahel rainfall is almost three times that explained by the eastern Pacific SSTs. It is demonstrated that a likely reason for this result is that the SST-associated vertical shears are more equatorially confined, so that the changes in shear in the main development region have a stronger association with the rainfall than with the SSTs.

## 1. Introduction

Most of the tropical cyclones in the North Atlantic basin (including the North Atlantic Ocean, the Caribbean Sea, and the Gulf of Mexico) form from easterly wave disturbances (e.g., Pasch and Avila 1994). The easterly waves have their origins over Africa, where their maximum amplitude is between 10° and 15°N (Reed et al. 1977). Most Atlantic tropical cyclones not spawned by these wave disturbances tend to form poleward of 25°N. The stages of a tropical cyclone include tropical depression [maximum sustained (1-min mean) surface wind $<18$ m s$^{-1}$], tropical storm (18–32 m s$^{-1}$), and hurricane ($\geq 33$ m s$^{-1}$). Hurricanes that have attained a maximum sustained surface wind speed of $\geq 50$ m s$^{-1}$ are referred to as major (or intense) hurricanes (MHs). The definition of MH (Hebert and Taylor 1979) corresponds to categories 3, 4, or 5 on the Saffir–Simpson scale (Simpson 1974).

Although the number of easterly waves in the tropical Atlantic tends to be fairly steady from year to year, the fraction of these that develop into tropical cyclones exhibits substantial interannual variability (Frank 1975; Pasch and Avila 1994). Not only the number but also the strength and location of the Atlantic basin tropical cyclones vary greatly from year to year (Neumann et al. 1993). The search for conditions that result in the development or nondevelopment of waves into tropical cyclones has been the subject of numerous studies, some of which have attempted to relate the variability to fluctuations in the tropical and global climate. Shapiro (1982a,b) was the first to establish statistically significant relationships between interannual variability of

*Corresponding author address:* Mr. Stanley B. Goldenberg, Hurricane Research Division, U.S. Department of Commerce/NOAA, 4301 Rickenbacker Causeway, Miami, FL 33149-1026.
E-mail: goldenberg@aoml.noaa.gov

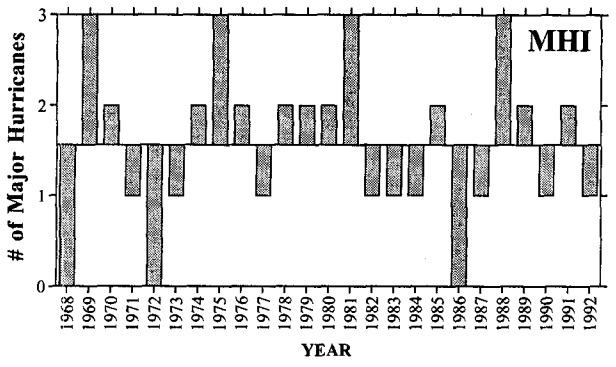


FIG. 1. Major hurricane index as defined by the number of August–October major hurricanes. Center horizontal reference line corresponds to sample (1968–92) mean.

Atlantic tropical cyclone activity and large-scale patterns of seasonally averaged sea level pressure (SLP), sea surface temperatures, and 500-mb heights for the Atlantic basin. Lower SLP and warmer SSTs in the Atlantic were found to be associated with more active seasons. In other studies, occurrences of strong El Niño events, the large-scale intrusions of anomalously warm water into the equatorial eastern Pacific, have been shown to be associated with suppressed Atlantic tropical cyclone activity (Gray 1984a,b; Shapiro 1987). Gray (1984a,b) also found a substantial predictive signal for the Atlantic hurricane season in the stratospheric quasi-biennial oscillation. More recently, Gray (1990) and Landsea and Gray (1992) have established a very significant relationship between above (below) normal rainfall in western Africa and above (below) normal Atlantic basin tropical cyclone activity. This relationship is particularly strong for MH activity.

It is well accepted that strong local vertical shear between the upper- and lower-tropospheric winds inhibits the formation and intensification of tropical cyclones (e.g., Gray 1968; Pasch and Avila 1992), probably as it relates to prevention of organization of deep convection. Modeling studies of tropical cyclogenesis confirm this effect (Kurihara and Tuleya 1981). As suggested by Gray et al. (1993), the Atlantic basin *in the mean* is not particularly favorable for tropical cyclone development. It appears that it is only during those years where conditions are such that the climatological shear is reduced that a substantial fraction of the systems can be expected to develop. Based on various studies such as Gray (1984a) and Shapiro (1987), it can be inferred that year-to-year changes in the large-scale environment have a substantial influence on the overall activity of each Atlantic hurricane season (see also Pasch and Avila 1994).

Gray (1984a) suggested that the relationship between El Niño and Atlantic basin tropical cyclone activity is due to changes in upper-level winds over the southern portion of the basin. He hypothesized that during an El Niño event, increased upper-level westerlies would help create unfavorable conditions for development by increasing vertical shear and by producing positive upper-level vorticity anomalies. Shapiro (1987) was able to confirm the increase in vertical shear resulting from a near-equatorial Walker-cell-type circulation but found unfavorable vorticity anomalies confined primarily to lower levels. Landsea and Gray (1992) showed that the 200-mb winds over the Caribbean basin are negatively correlated with west African rainfall. In particular, above-normal rainfall was associated with easterly wind anomalies at 200 mb, which reduced the vertical shear in that region. In addition, they suggested that part of the relationship between African rainfall and MH activity is due to variations in both the amplitude and amount of deep convection of the easterly waves—that is, that the waves are "stronger" during wet years, so that more of them develop. In spite of the strong association between West African rainfall and overall MH activity, however, Gray and Landsea (1992) and Landsea et al. (1992) have indicated that major hurricanes affecting the Gulf Coast show little relationship to fluctuations in West African rainfall, probably due to the relatively higher number of systems of noneasterly wave origin impacting the Gulf Coast. More recently, Gray (1994) also provided evidence for an out-of-phase relationship between Atlantic hurricanes forming to the north and south of 25°N.

The vast majority of the deadliest and costliest hurricanes of this century to affect the United States were MHs (Hebert et al. 1993). Although MHs account for only 20% of the landfalling U.S. tropical storms and hurricanes, they account for over 70% of the damage (Landsea 1993).[1] There are several other reasons for the choice of MH activity as the measure of Atlantic basin activity. Landsea (1991) demonstrated that MH frequency exhibits a much stronger interdecadal variability than all hurricanes or hurricanes and tropical storms combined. The interannual variability for MHs for the period 1944–91 is more than twice than that for hurricanes and storms together (Landsea 1993). In addition, of the various measures of Atlantic basin tropical cyclone activity, MHs show one of the strongest correlations with African rainfall (Landsea and Gray 1992). The physical mechanisms responsible for this relationship have not, however, been completely established.

The purpose of the present study is to further elucidate these various associations by using linear correlations to examine contemporaneous relationships between interannual tropical cyclone variability and

[1] Note that Hurricane Andrew (1992) statistics were not in the Landsea (1993) study. The $20–25 billion worth of damage from Andrew (Mayfield et al. 1994) would increase the MH damage contribution to more than 75%.

selected measures of the large-scale circulation. Specifically, the relationships between MHs and indices of El Niño, West African rainfall, and upper- and lower-level tropospheric winds, including vertical shear, are examined. Partial correlations are used to isolate some of the physical mechanisms responsible for variations in MH activity.

In section 2, the data used in the current study are described and linear correlations between indices for MH activity, El Niño, and West African rainfall are presented. Linear correlations between the indices and the winds are presented in section 3. Statistical significance of the correlations is evaluated. The method of partial correlations is used in section 4 to isolate some of the physical mechanisms responsible for the various relationships. The results are discussed in section 5.

## 2. Data description

### *a. MH index*

The source for the tropical cyclone parameters used in this study is the Tropical Prediction Center (TPC, formerly the National Hurricane Center)/National Oceanic and Atmospheric Administration (NOAA) best track file for the Atlantic basin (Jarvinen et al. 1984). Although these data are available since 1886, only the data for the years since 1944, when routine aircraft reconnaissance of Atlantic tropical cyclones began, are considered very reliable. The greatest reliability starts around the mid-1960s, when satellite detection of Atlantic tropical cyclones began operationally (Neumann et al. 1993). The length of record in the present study is limited by the availability of the large-scale wind data, described in section 2b, which only extend back to 1968. Therefore, the analyses in this study utilize only the years with the most reliable tropical cyclone data.

Landsea (1993) documented that hurricanes in the 1940s to the 1960s were assigned slightly higher maximum sustained surface wind speeds for a particular minimum central surface pressure than hurricanes from 1970 to 1991 with the same central pressure. This bias is as high as 5 m $s^{-1}$ for category 4 and 5 hurricanes. At the threshold value for MHs of 50 m $s^{-1}$, the bias appears to be ~2.5 m $s^{-1}$. Therefore, consistent with the bias adjustment from Landsea (1993) and the use of this adjustment in Gray et al. (1994), 52 m $s^{-1}$ is used for the present study as the threshold for MHs before 1970.

Although the North Atlantic hurricane season lasts officially from June through November, for the period from 1886 to 1991 more than 95% of all MHs occurred during August, September, and October (ASO) (Landsea 1993); for 1968–92 all but one MH occurred during these months. The MH index (MHI) for the present study, the number of MHs during ASO for each year, is shown in Fig. 1 for the period 1968–92. The bias adjustment has reduced the number of MHs in 1969 by 2. The 25 years comprise a relatively inactive period, with the MHI ranging from 0 to 3 with a mean of 1.6. By contrast, during the preceding 25 years, 1943–67, the MHI was *more than* 3 for 6 of the years and the mean was 2.6. During most of the years during the period 1968–92, a drought persisted in the Sahel. The relationship between this drought and the lower-than-normal number of MHs has been discussed in detail by Gray (1990) and Landsea and Gray (1992).

As noted by Landsea (1993), more than 80% of the depressions that develop into MHs come from easterly waves that originate over Africa. Figure 2 identifies the precursor systems[2] and development locations of all MHs during ASO for 1968–92. Note that 34 of the 39 MHs for that period formed from easterly waves. Figure 2 also shows the complete tracks (depression stage and stronger) for all of the MHs for this period. Note as well that 29 of the MHs in this period develop from depressions that formed between 9° and 20°N. In the present study, the band where most of the systems begin to develop, from ~10° to 20°N between the west coast of Africa and Central America, will be referred to as the "main development region." There were several easterly waves that reached depression stage north of this region (see Fig. 2), but all of the depressions that developed in the main development region formed exclusively from easterly waves.

### *b. Wind analyses*

Monthly mean wind data derived from the National Centers for Environmental Prediction's (NCEP, formerly the National Meteorological Center) final tropical strip wind (1968–74)[3] and global analyses (1974–92) were obtained from the National Center for Atmospheric Research. The tropical and global monthly analyses, with resolutions of 5° latitude by 5° longitude and 2.5° latitude by 2.5° longitude, respectively, were interpolated using a bicubic spline algorithm to a 1° latitude by 1° longitude grid. Upper-level winds are represented by the 200-mb analyses. In order to evaluate the low-level flow for as long a record as possible, 700-mb winds are used. While winds for the 850-mb level are only available back to 1975, the 700-mb winds are available back to 1968. Several correlations

[2] The origins of the MHs for each year were obtained from the yearly Atlantic hurricane season (e.g., Pasch and Avila 1992) and Atlantic tropical systems (e.g., Pasch and Avila 1994) summaries appearing in *Monthly Weather Review*. These were supplemented by information from the appendix of Hess (1994).

[3] Missing wind data for October and November 1972 were filled in by linearly interpolating the anomalies from September and December 1972 and adding them to the climatology for the missing months.

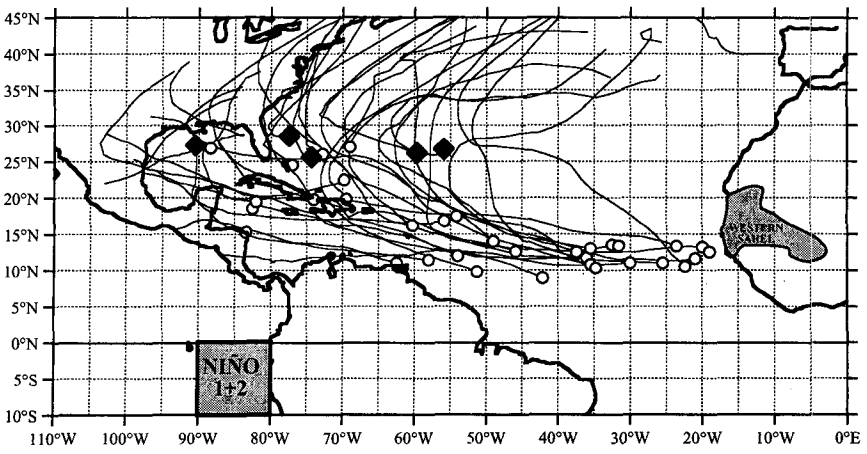


FIG. 2. Complete tracks (for tropical depression stage and stronger) of all North Atlantic basin tropical cyclones that reached major hurricane strength during ASO for 1968–92. Open circles and filled diamonds mark the locations where the systems of easterly wave and noneasterly wave origin, respectively, initially reached depression strength. The Niño 1 + 2 region and the region in the western Sahel that contains the rainfall stations used by Landsea and Gray (1992) to derive the Sahelian rainfall index are also indicated.

from this study using 700-mb level winds have also been recalculated for 1975–92 and compared to correlations using 850-mb level winds for the same period. The results are virtually identical, with the correlations using the 850-mb level winds being slightly stronger than those using the 700-mb level winds. Various analysis techniques, described by Arkin (1982) and Dey (1989), were utilized by the NCEP during the 25-year period considered here. In order to examine the possible impact of the changes in analysis techniques on the correlations presented in this study, results using NCEP winds for 1975–92 were compared to those using winds generated by a single analysis scheme archived by the TPC (see discussion in Shapiro 1987). The correlations in sections 3 and 4 using the NCEP and TPC winds display only minor differences. The 25-year wind record, 1968–92, used in the present study is more than twice as long as that used by Shapiro (1987).

Winds averaged for ASO during the 25-year period of 1968–92 are shown in Fig. 3. The mean upper-level winds (upper panel) are westerly over most of the Atlantic basin. The lower-level flow (middle panel) is easterly from the equator to close to 30°N. The net vertical shear $V_z$ (lower panel), the difference between the upper- and lower-level winds, is westerly throughout almost the entire basin. The largest magnitudes of the vertical shear $|V_z|$ in the Tropics and subtropics lie along an axis from ~15°N in the Caribbean Sea to ~20°N at the west coast of Africa. This area of strong shear (>10 m s$^{-1}$) covers most of the main development region for Atlantic tropical cyclones. Hebert (1978) suggested that the vertical shear in the vicinity of a tropical system that is south of ~30°N needs to be less than ~5 m s$^{-1}$ for tropical cyclone development to occur.[4] Therefore, as noted above, the mean conditions in the main development region tend to be unfavorable for development.

Of course the day-to-day values for $|V_z|$ would be expected to vary substantially from the three-month climatological values in Fig. 3. Intermonthly variations occur as well. In particular, during the "late season" month of October, $|V_z|$ in the main development region is usually larger than during August and September, the other two months in the seasonal average used here. Of the 11 MHs that have formed in October since 1949, however, almost all formed from easterly waves and began development (reached depression strength) in the main development region, just as in August and September. Some of the correlations in sections 3 and 4 were also calculated using only August and September data to test for the sensitivity of the inclusion of October in the seasonal average and showed only minor differences. Therefore, consistent with the perspective of previous hurricane climate studies (see section 1), the present study will use mean winds for ASO in an attempt to evaluate the overall characteristics of each hurricane season.

### c. *El Niño index*

Gray et al. (1993) use Climate Prediction Center (CPC, formerly the Climate Analysis Center)/NOAA

[4] The threshold used in Hebert (1978) was for the difference between analyses for the upper (200–600 mb) and lower (600–1000 mb) layers. For the difference between the 200- and 700-mb levels used to specify $V_z$ in the present study, an equivalent threshold for development might be somewhat higher.

values for the Niño 3 region (5°N–5°S, 150°W–90°W) for June–July in making their 1 August forecast of Atlantic basin tropical cyclone activity. For the present study, anomalies (based on 1950–79 climatology) from the Geophysical Fluid Dynamics Laboratory (GFDL)/NOAA SST dataset, described by Oort et al. (1987), were averaged over the Niño 1 and Niño 2 (Niño 1 + 2; see Fig. 2), and Niño 3 and Niño 4 (5°N–5°S, 160°E–150°W) regions. The GFDL SST analyses are only available through 1988; anomalies for later years have been obtained using the SST anomalies derived by the CPC/NOAA for the same areas.[5] The monthly CPC anomalies have been adjusted to account for the difference between the GFDL and CPC climatologies for the various regions. Linear correlations have been calculated between six of the measures of tropical cyclone activity for the North Atlantic basin, such as those used by Gray et al. (1993) for ASO and ASO SST anomalies for the Niño regions for the period 1968–92. The nature of these relationships may not necessarily be valid for earlier periods. In particular, Wang (1995) indicates that the character of the temporal and spatial evolution of the tropical Pacific SST anomalies related to El Niño episodes changed in the mid-1970s. For the time period of the present study, of the various regions, the anomalies for Niño 1 + 2 demonstrated the strongest contemporaneous correlation with all but one of the measures of tropical cyclone activity and, therefore, will be used as the contemporaneous quantitative measure of El Niño. Some of the correlations presented in this study were also calculated using the anomalies for the Niño 3 and Niño 4 regions and yielded similar results.

The El Niño index (ENI), derived from the Niño 1 + 2 region anomalies and averaged for ASO, is shown in Fig. 4. The period used for this study encompasses several El Niño events described in Quinn et al. (1987): the "very strong" 1982–83 event, the "strong" 1972–73 event, and the "moderate" 1976 and 1987 events. Also included are the "weak" 1969 event (Quinn et al. 1978) and the more recent 1992 event (Wang 1993). For the purpose of the contemporaneous correlations presented in this study, it should be noted that the actual maximum strength of a particular event (usually during spring) is not used, but rather the anomaly during ASO, the active portion of the Atlantic hurricane season. The strongest ASO anomalies are for the strong 1972 and very strong 1982–83 events. Note, however, that the SST anomaly had already become strongly negative by ASO of the second year of the 1972–73 event, whereas the 1982–83 event still displays a positive anomaly in its second year, 1983. In addition, the ASO anomaly for 1992 is slightly negative even though El Niño conditions accompanied by positive anomalies in the Niño 1 + 2 region had existed earlier that year. The moderate 1976 and 1987 events also display positive anomalies in excess of 1°C.

### *d. West African (Sahelian) rainfall index*

The Sahel, located between ~10° and 20°N in Africa, receives most of its precipitation during the Northern Hemisphere's summer monsoon season. Landsea and Gray (1992) have correlated rainfall amounts at individual stations with North Atlantic MH activity and created a rainfall index for the western Sahelian region for June–September. The stations used for this Sahel index (SI) are from the region delineated in Fig. 2. The values for SI for 1968 through 1992 (Landsea and Gray 1992; C. Landsea 1992, personal communication) are shown in Fig. 5. The June–September period used for SI is not strictly contemporaneous with the ASO period used in the present study. This rainfall index constitutes, however, the rainfall parameter concurrent with the Atlantic hurricane season used in Gray (1990), Gray and Landsea (1992), and Landsea and Gray (1992). Also, as presented in Table 4 of Landsea and Gray (1992), almost two-thirds of the western Sahelian rainfall during June–September occurs during August and September, and little rainfall occurs during October.

During most of the years used for the present study, the Sahel experienced rainfall below the long-term mean (1949–90) due to the drought that began in 1968 (Lamb 1982). Only 3 years since that time have exhibited rainfall amounts above the long-term mean. The 19 driest years from 1949–90 in the Landsea and Gray (1992) study are all contained in the 25-year period used here. The years in the present study still exhibit substantial interannual variability, however, as evidenced in Fig. 5. In addition, Landsea and Gray (1992) showed that the correlation between MH activity and the SI is about the same for the "wet" (1949–69) and "dry" (1970–90) periods used in their study, indicating a very stable relationship that is probably still valid during the drier decades. However, because a substantial portion of SI (and MHI) variability occurs on the decadal timescale (Landsea 1991), it is possible that the relationships elucidated in this study would be different for the wetter decades such as the 1950s and 1960s.

### *e. Correlations*

The linear correlation coefficients and corresponding reduction of variance for the relationships between MHI, ENI, and SI are given in Table 1. A classical runs test for serial correlation (e.g., Siegel 1956; cf. Shapiro 1984, footnote on p. 1382) indicates that the series MHI, ENI, and SI are each nearly random during the 25-year record. Correlations in this study will be termed "significant" if their magnitude exceeds the 95% signifi-

[5] Since the time of this study, the GFDL dataset has been extended through 1992 and the CPC indices have been extended back to 1950.

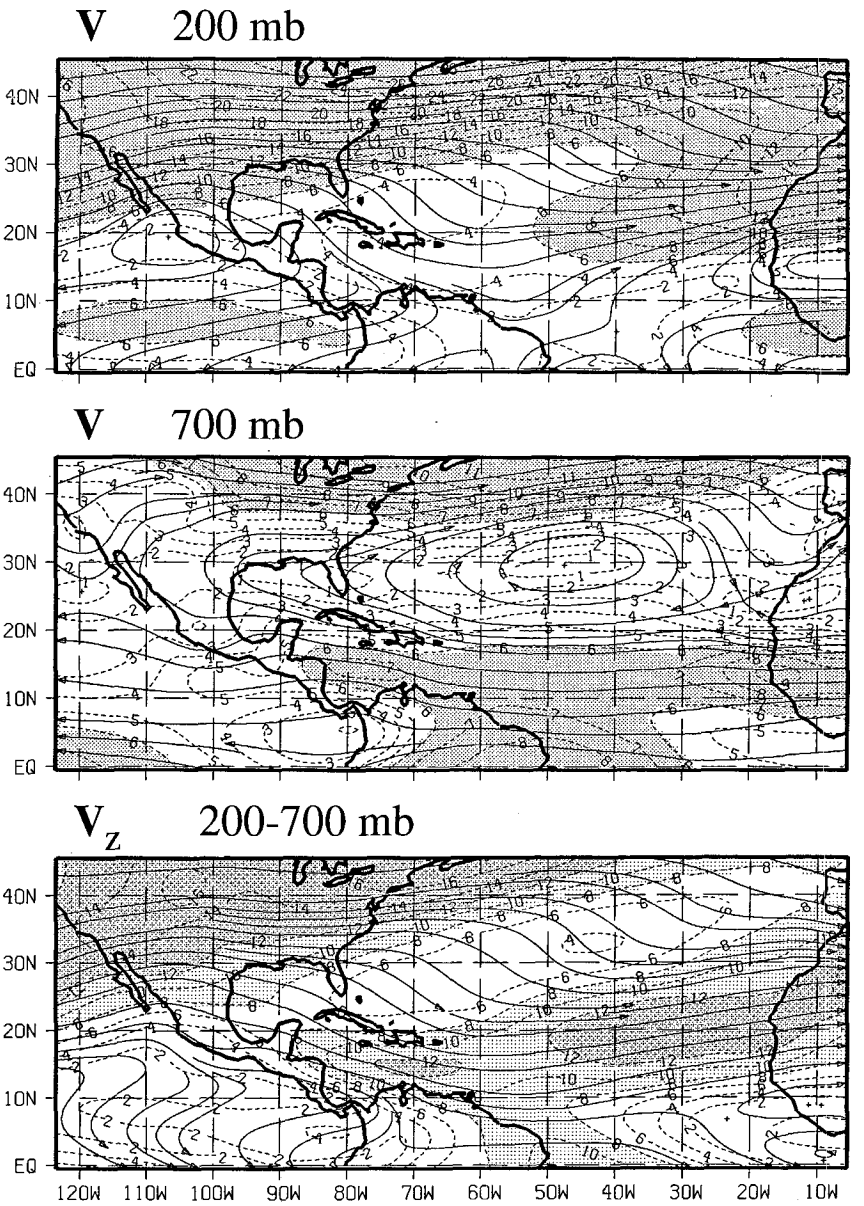


FIG. 3. Average ASO winds from the NCEP analyses for 1968–92. Streamlines and isotachs (m $s^{-1}$) are shown. Isotach intervals are 2 m $s^{-1}$ (200 mb and $V_z$) and 1 m $s^{-1}$ (700 mb). Wind speeds >6 m $s^{-1}$ (200 and 700 mb) and >8 m $s^{-1}$ ($V_z$) are shaded.

cance level for a sample size of 25, as determined from the appropriate $F$ test (e.g., Kleinbaum and Kupper 1978). The (small) linear trend has been removed from each time series prior to computing the correlations.

The linear correlation coefficient between MHI and ENI is $r$(MHI, ENI) = −0.41. This negative correlation, explaining 17% of the variance, indicates that, as shown by previous studies, MH activity tends to decrease when there are positive SST anomalies in the equatorial eastern Pacific. The linear correlation coefficient between MHI and SI is $r$(MHI, SI) = 0.70. This positive correlation, explaining 49% of the variance, indicates that MH activity tends to increase during anomalously high Sahelian rainfall and decrease during drought (Gray 1990; Landsea and Gray 1992).

## 3. Results for primary relationships

### *a. Correlation of MHI with winds*

The map of the linear correlation coefficients between MHI and $|V_z|$, $r$(MHI, $|V_z|$), is shown in Fig. 6. The

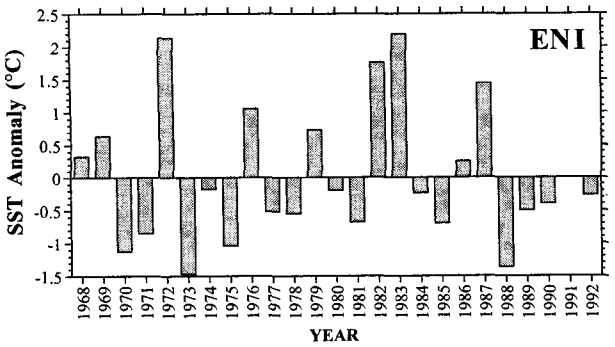


FIG. 4. El Niño index as defined by the average SST anomalies during ASO for the Niño 1 + 2 region (see Fig. 2).

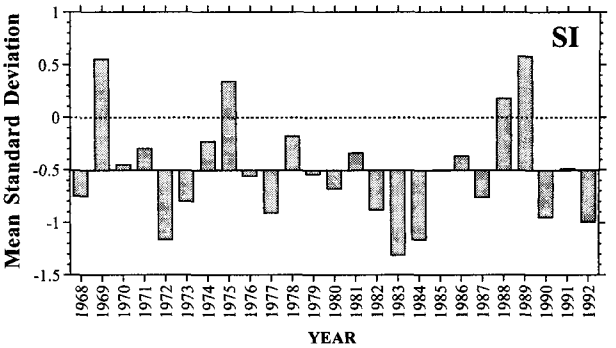


FIG. 5. June–September Sahelian rainfall index in units of mean standard deviations, as derived by Landsea and Gray (1992) for the region delineated in Fig. 2. Solid horizontal reference line corresponds to sample (1968–92) mean. Horizontal dotted line indicates long-term (1949–90) mean.

magnitude of the vertical shear $|V_z|$ has been calculated for each year after $V_z$ has been averaged for ASO. Regions in Fig. 6 where the correlations are significant, based on an a priori test, are shaded. Since the discussion of the significant correlations will be confined primarily to the main development region, where relationships between winds and the MHI are expected on physical grounds, an a priori test is appropriate. It should be noted that because of the winds' spatial scales of variability and teleconnection patterns, a region might contain strong correlations not because that region is in itself physically related to Atlantic tropical cyclone development, but rather because the winds in the region are correlated with the winds in a physically significant area.

The correlations are negative to the south of 20°N throughout almost all of the Atlantic basin. The strongest correlations, accounting for up to 50% of the variance, are between ~10° and 15°N, directly off the West African coast and in the central portion of the basin. Most of the systems that developed into MHs during the period 1968–92 reached depression stage between ~10° and 15°N (see Fig. 2), basically the region where the magnitude of the correlations exceeds 0.6. The negative correlations in this region indicate that the number of MHs tends to be above (below) average for years where $|V_z|$ in the main tropical cyclone development region is bel^w (above) the climatological mean. The correlations in Fig. 6 are similar to those found by Shapiro (1987). In the seasonal forecasts issued on 1 August, Gray et al. (1993) use 200-mb zonal wind anomalies in the eastern Caribbean, one of the regions shown here to have the strongest correlations.

### b. *Correlation of ENI with winds*

The negative correlation between the MHI and the ENI (Table 1) has been attributed to El Niño being associated with upper-level westerly anomalies over the Caribbean and tropical Atlantic, resulting in increased vertical shear (Gray 1984a; Shapiro 1987). Figure 7 shows the linear correlation coefficients between the ENI and $|V_z|$, $r(\text{ENI}, |V_z|)$. The scalar covariances (not shown) for this relationship associated with the positive correlations between 10° and 15°N are 1–2 m s$^{-1}$. As might be expected, the correlations are strongest in the southwest portion of the Atlantic basin, the region closest to the anomalous warm waters in the equatorial eastern Pacific associated with El Niño. The correlations are positive for most of the basin south of 20°N, with some regions explaining over 50% of the variance. A positive correlation signifies that a positive ENI (anomalously warm SST, such as would be associated with an El Niño event) is associated with increased $|V_z|$ in the main tropical cyclone development region. This supports the findings of other studies that during an El Niño event, hurricane formation is inhibited due to increased vertical shear in the main development region. The southern portion of the pattern in Fig. 7 is similar to the changes in vertical shear associated with another El Niño index in Shapiro (1987).

To examine the circulation features that produce the association between the ENI and $|V_z|$ shown in Fig. 7, vector correlations and covariances were calculated for the relationships between the ENI and the upper-level, lower-level, and vertical shear vector winds. The covariance vector, showing the portion of the wind variability correlated with the ENI, is given by

$$C(\text{ENI}, V) \equiv \sigma_u r(\text{ENI}, u)i + \sigma_v r(\text{ENI}, v)j, \quad (1)$$

TABLE 1. Linear correlation coefficients for relationships between the MHI, ENI, and SI. Partial correlation coefficients and multiple correlation coefficients are also shown. Correlations that are significant at the 95% level are marked with an asterisk.

| | $r$ | $r^2$ |
|---|---|---|
| $r$(MHI, ENI) | −0.41* | 0.17* |
| $r$(MHI, SI) | 0.70* | 0.49* |
| $r$(ENI, SI) | −0.43* | 0.19* |
| $r$(MHI, ENI\|SI) | −0.16 | 0.03 |
| $r$(MHI, SI\|ENI) | 0.64* | 0.41* |
| $R$(MHI; ENI, SI) | 0.71* | 0.50* |

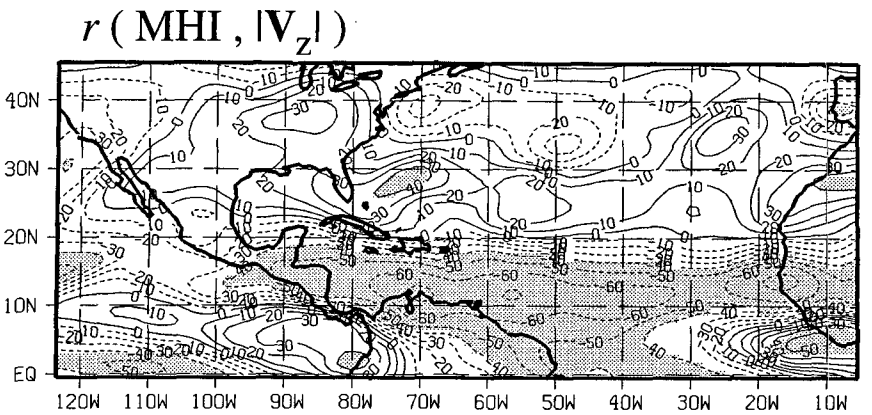


FIG. 6. Map of linear correlation coefficients between the MHI and $|V_z|$ for 1968–92. Magnitudes are multiplied by 100; contour interval is 0.1. Negative contours are dashed. Regions where the correlations are significant at the 95% significance level (see text) are shaded.

where $u$ and $v$ are the zonal and meridional wind components, respectively; $\sigma_u$ and $\sigma_v$ are the standard deviations of the wind components; and $i$ and $j$ are the zonal and meridional unit vectors, respectively. The covariances indicate wind anomalies associated with ENI anomalies one standard deviation above normal. The statistically significant portions of the patterns for the correlation and covariance fields for the upper and lower levels (not shown) are qualitatively similar to results shown in Shapiro (1987), with an equatorially confined, near-zonal circulation. In the covariance fields for the present study, westerly anomalies at the 200-mb level extend across the entire analysis region, including the east Pacific, from the equator to ~20°N, with the strongest anomalies in the southwest portion of the Atlantic basin. The lower-level (700 mb) covariances contain easterly anomalies extending across most of the analysis region from the equator to ~15°N. Although the magnitudes of the covariances at the lower level are much less than for the upper level in most of the southern portion of the basin, the correlations for the region containing the lower-level easterlies are nevertheless statistically significant. The map of the covariances for the relationship between the ENI and $V_z$, $C(\text{ENI}, V_z)$, is shown in Fig. 8. The upper- and lower-level anomalies associated with a positive (warm) ENI value combine to create strong westerly shear anomalies throughout the entire basin south of 20°N. These westerly anomalies add to the climatologically westerly vertical shear in the Atlantic basin (see Fig. 3) and result in a region of increased $|V_z|$ (as shown in Fig. 7), thereby creating an environment less favorable for tropical cyclone development south of 20°N.

A zero correlation line in Fig. 7, associated with a change in direction of the shear anomalies in Fig. 8, lies east–west along 20°N from the coast of Africa to the eastern tip of Cuba; in the Gulf of Mexico it lies close to 25°N. An area of negative correlations occupies the region over the Atlantic north of the zero line to between ~30° and 35°N, where the direction of the

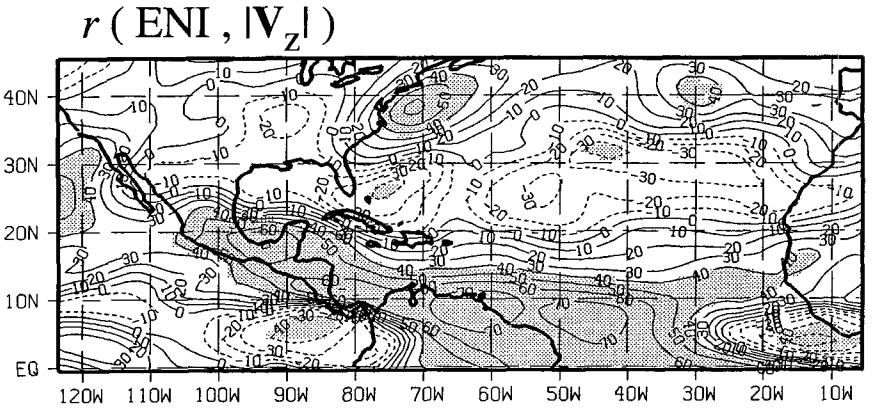


FIG. 7. Same as Fig. 6 but for the correlation between the ENI and $|V_z|$.

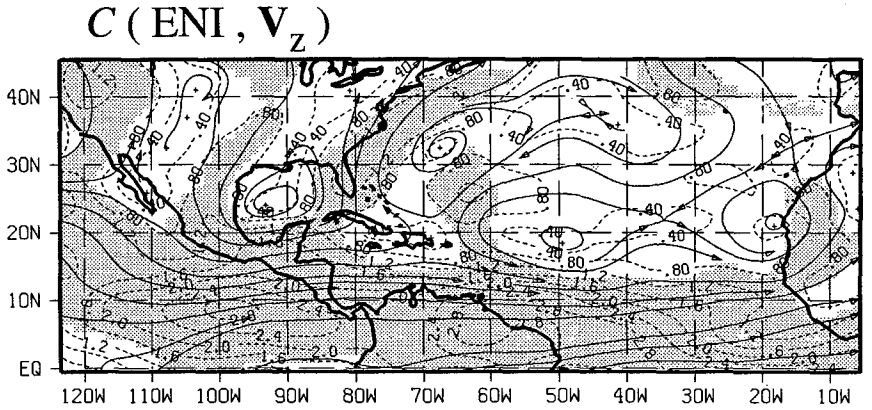


FIG. 8. Covariances for the relationship between the ENI and $V_z$ for 1968–92. Streamlines and isotachs (m $s^{-1}$) are shown. Isotach interval is 0.4 m $s^{-1}$. Regions where the linear correlations for the relationship (based on the multiple correlation using both wind components) are significant at the 95% level are shaded. The threshold for the significance level is based on correlations with only one wind component since the covariances in the main region of significant correlations, south of about 15°N, are nearly zonal.

shear anomalies again changes. Negative correlations signify that a positive ENI is associated with reduced $|V_z|$ in that region. Although almost none of these negative correlations are statistically significant, the pattern suggests that changes of $|V_z|$ in this band to the north of the main development region are unrelated to, or possibly out of phase with, changes in $|V_z|$ south of 20°N. The correlation between area-averaged $|V_z|$ to the north and to the south of 20°N is, in fact, slightly negative but is not statistically significant. Note that Fig. 6, which showed $r(\text{MHI}, |V_z|)$, has a similar sign-reversal area to the north of 20°N. Since the main physical mechanism for SST-associated $|V_z|$ variability is from an equatorially confined zonal circulation, it would be expected that $|V_z|$ fluctuations to the north would have a weaker, or in this case even opposite, relationship. The potential importance of the sign-reversal area will be discussed further in section 5.

Vorticity anomalies associated with the upper- and lower-level anomalies that contribute to vertical shear, shown in Fig. 8, may also contribute to the relationship between the MHI and the ENI. The vertical component of the vorticity, defined here as $\zeta[C(\text{ENI}, V)] \equiv \mathbf{k}\cdot\nabla \times [C(\text{ENI}, \mathbf{V})]$, where $\mathbf{k}$ is the vertical unit vector, has been calculated for the covariance fields discussed above. The results for vorticity (not shown) are similar to the results presented in Shapiro (1987). Cyclonic anomalies in the upper troposphere and anticyclonic anomalies in the lower troposphere cover most of the main tropical cyclone development band. Gray (1984a) hypothesized that part of the cause for the suppression of North Atlantic tropical cyclone activity during El Niño events was due to 200-mb level cyclonic vorticity anomalies. The results from the present study are consistent with this hypothesis and also indicate possible contributions to the El Niño–MH relationship from anticyclonic vorticity in the lower level.

### c. *Correlation of SI with winds*

The correlations between the SI and $|V_z|$, shown in Fig. 9, are negative for most of the basin south of 25°N, with some regions explaining over 40% of the variance. Statistically significant correlations cover most of the main development region. As with the ENI, the vertical shear scalar covariances with the SI (not shown) are between ~1 and 2 m $s^{-1}$ across almost this entire region. The negative correlations signify that increased (decreased) western Sahelian rainfall is associated with decreased (increased) $|V_z|$. As suggested by Gray (1990), this relationship implies that one of the reasons for increased (decreased) MH activity during years with an increased (decreased) SI is the associated decreased (increased) vertical shear.

To illustrate the cause of the fluctuations in $|V_z|$ associated with the SI, correlations and covariances have been calculated for the relationships between the SI and the upper-level, lower-level, and vertical shear vector winds. The covariances for these relationships are shown in Fig. 10. At the 200-mb level (top panel of Fig. 10), easterly anomalies extend across the entire analysis region from the equator to ~20°N. The increased upper-level easterlies in the main development region associated with an increased SI support the findings of Landsea and Gray (1992), using station data in the Caribbean Sea area. In addition, at the lower level (700 mb, middle panel) westerly anomalies extend across most of the analysis region from the equator to close to 20°N. In certain portions of the central Atlantic, the upper- and lower-level anomalies are of similar mag-

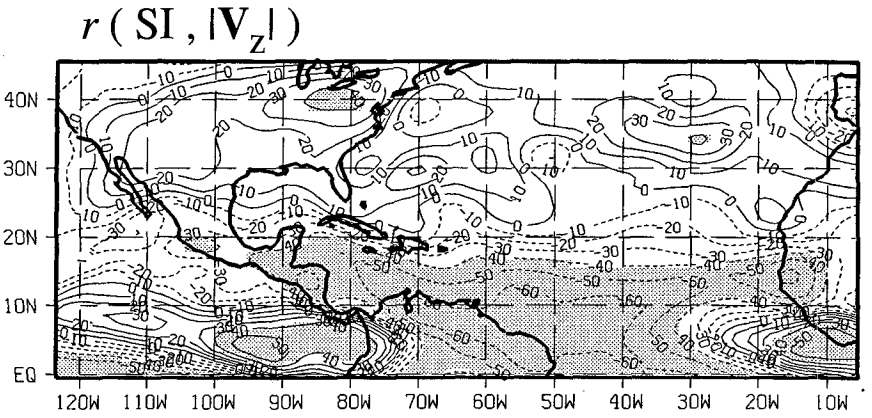


FIG. 9. Same as Fig. 6 but for the correlation between the SI and $|V_z|$.

nitude. In fact, although the magnitudes of the covariances at the lower level are less than those for the upper level in most of the southern portion of the basin, the correlations (not shown) for the region containing the lower-level westerlies are stronger than those for the upper level, explaining over 50% of the variance in the area centered on 10°N and 50°W. These findings indicate that the lower-level wind fluctuations associated with SI fluctuations are also important contributors to changes in vertical shear in the main development region.

The upper- and lower-level anomalies associated with positive (wet) SI anomalies form an equatorially confined, near-zonal circulation that results in strong easterly vertical shear anomalies (bottom panel) across the entire basin south of ~20°N, just as would be associated with negative (cold) ENI anomalies (cf. Fig. 8). The easterly anomalies associated with a wet SI and a cold ENI cancel part of the climatological westerly vertical shear in the Atlantic basin (see Fig. 3), thereby creating an environment more favorable for tropical cyclone development, just as the westerly anomalies associated with a negative (dry) SI and a positive (warm) ENI add to the climatological shear, resulting in increased $|V_z|$. During drought years, the climatological easterly jet at 200 mb located in the southeast corner of the domain in Fig. 3 (top panel) is weakened by westerly upper-level anomalies. The climatological easterly jet at 700 mb in Fig. 3 (middle panel) located just to the north of the 200-mb jet would be strengthened by lower-level easterly anomalies during the drought years. These variations in the upper- and lower-level jets are consistent with the findings of Newell and Kidson (1984).

The spatial extent of the wind and shear covariance patterns with the SI (Fig. 10) and the ENI (see Fig. 8) makes it quite unlikely that the correlations and covariances shown here are solely the result of wind anomalies caused by tropical cyclones during the ASO period. The shear anomalies, in particular, are strongest south of 10°N and extend westward over South America into the east Pacific. Moreover, lag covariances between the ENI, as well as the SI, and vertical shears in June–July (not shown) evidence similar patterns.[6] Thus, in agreement with Shapiro's (1987) monthly analysis for tropical storms, a favorable environment in the main development region appears to be established several months prior to the time when MHs develop.

In the map of correlations between the SI and $|V_z|$ in Fig. 9, there are only negligible statistically significant regions to the north of the main development region. The correlations to the north are small and generally positive. As with the ENI (Fig. 7), the correlation changes sign where the direction of the shear covariances (Fig. 10) changes. The different nature of the correlations to the north was discussed earlier, with respect to the relationship between the ENI and $|V_z|$ (see section 3b). The potential impact of the conditions in that region will be discussed further in section 5.

As with the ENI, vorticity anomalies associated with the circulation patterns may also contribute to the relationship between MH activity and the SI. In the case of these SI-associated patterns, anticyclonic anomalies in the upper troposphere and cyclonic anomalies in the lower troposphere (not shown) cover most of the main development region. These results suggest that, as with the association between MHs and the ENI, vorticity anomalies may also play a role in the associations between MHs and the SI, acting to favor development during wet years and inhibit development during drier years, as suggested by Landsea and Gray (1992).

## 4. Isolation of physical mechanisms

### *a. Separating influences of the ENI from the SI*

As discussed previously, the correlation between the MHI and the ENI is small and negative, but statistically

[6] As noted by Gray et al. (1993), early season (June–July) Atlantic tropical cyclone activity constitutes only a small portion of and has little relationship to the total activity of each season.

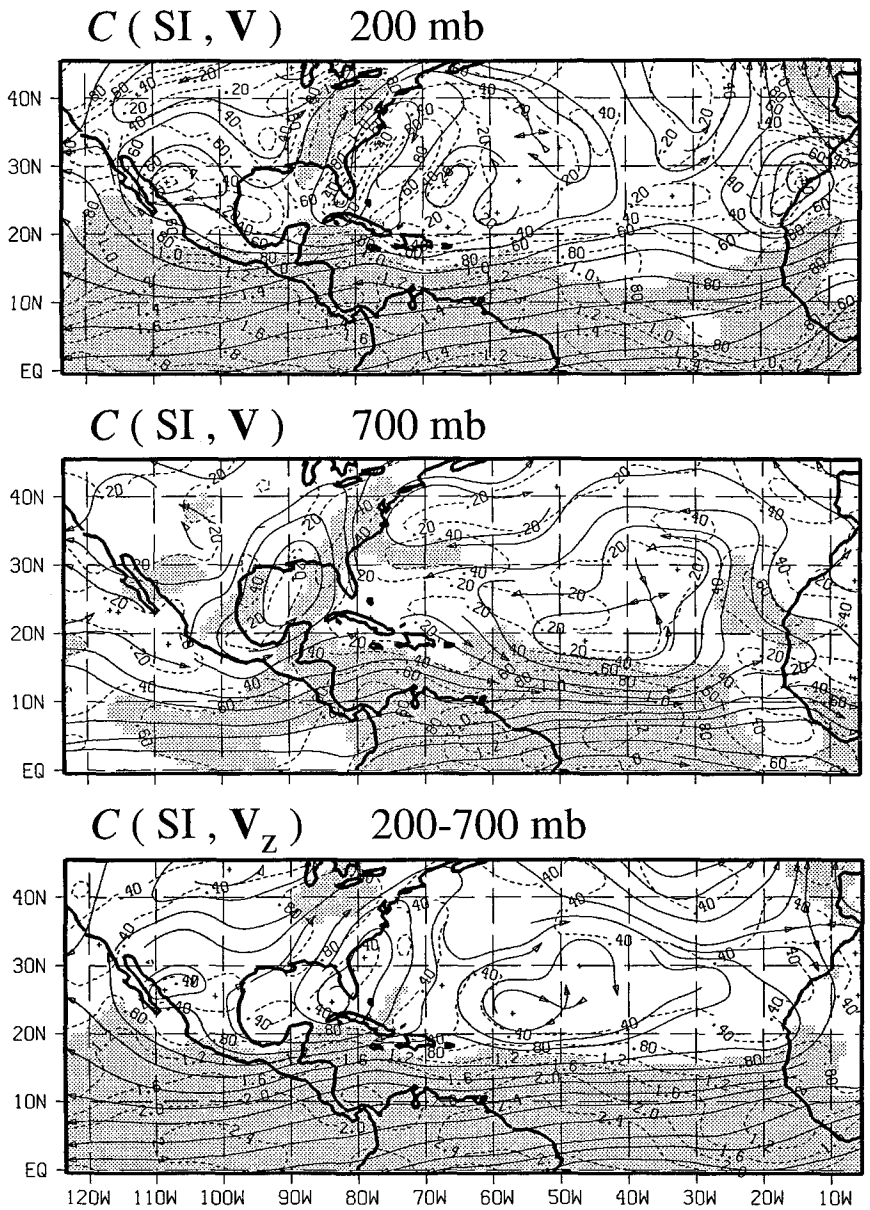


FIG. 10. Same as Fig. 8 but for the relationship between the SI and winds (isotach interval 0.2 m $s^{-1}$), as well as $V_z$ (isotach interval 0.4 m $s^{-1}$).

significant (see Table 1). The correlation between the MHI and the SI is large, positive, and also significant. The correlation between the ENI and the SI, $r$(ENI, SI) = −0.43, which is small but statistically significant, explains 19% of the variance. The relationship between El Niño and West African rainfall has also been discussed by Folland et al. (1986, 1991), Landsea et al. (1993), and others.

In order to separate the various factors related to interannual fluctuations of MHs, we use the method of partial correlations (see, e.g., Kleinbaum and Kupper 1978). The partial correlations involving the MHI, ENI, and SI are given in Table 1. The partial correlation coefficient between the MHI and the SI with the variability explained by the ENI removed, $r$(MHI, SI|ENI), is 0.64. This correlation is statistically significant and explains 41% of the remaining variance. Therefore, knowledge about the SI adds important additional information about MH activity apart from relationships with the ENI. The partial correlation coefficient between the MHI and the ENI with the variability explained by the SI removed, $r$(MHI, ENI|SI),

is, however, only −0.16. This correlation is not significant and explains less than 3% of the remaining variance. These results suggest that while the SI provides substantial information about interannual MH activity apart from associations with the ENI, the ENI supplies no significant additional independent information on contemporaneous fluctuations in MH activity above that already supplied by knowledge of the SI within the linear context. These results, of course, do not necessarily apply to nonlinear or predictive relationships.

To illustrate the probable reasons for these results, partial correlations and covariances were calculated with the winds. These partials isolate the relationship between the SI and the winds and the relationship between the ENI and the winds from those due to interrelationships between the SI and the ENI. Figure 11 shows the covariances for the relationships between the SI and the upper-level, lower-level, and vertical shear vector winds with the variability explained by the ENI removed. The covariances are given by

$$C(\mathrm{SI}, V|\mathrm{ENI}) = \sigma_u^*[r(\mathrm{SI}, u|\mathrm{ENI})]i + \sigma_v^*[r(\mathrm{SI}, v|\mathrm{ENI})]j, \quad (2)$$

where $\sigma_u^* = [1 - r^2(u, \mathrm{ENI})]^{1/2}\sigma_u$ and $\sigma_v^* = [1 - r^2(v, \mathrm{ENI})]^{1/2}\sigma_v$ are the standard deviations of the respective wind components after the variability explained by the ENI has been removed. Comparisons with Fig. 10 show how both the covariance and area of statistically significant correlations in the main development region at the 700-mb level (middle panel) are changed very little by the removal of the variability associated with the ENI. The results at the 200-mb level (top panel), however, show a noticeable reduction of covariance and area of significant correlations in the development region. This reduction suggests that much of the variability attributed to the relationship between the SI and the winds at 200 mb is actually due to the relationship between the SI and the ENI and, subsequently, the relationship between the ENI and the 200-mb winds. There is still evidence of an equatorially confined upper- and lower-level zonal circulation in Fig. 11, but the new results portray nearly equal contributions to the vertical shear anomalies (bottom panel) from the upper- and lower-level winds, whereas the contribution in Fig. 10 from the upper level was larger over most of the region. While Landsea and Gray (1992) focused primarily on the correlations with upper-level winds, the present results indicate the importance of low-level winds in understanding the changes in vertical shear in the main development region responsible for the relationship between the SI and MHs.

By contrast, removing the variability associated with the SI from the correlations and covariances between the ENI and the winds (not shown) does not noticeably reduce the region of significant correlations between the ENI and the winds at the upper or lower levels in the Atlantic basin. The covariance between the ENI and the winds is reduced more at the lower level than at the upper level, acting to slightly increase the dominance of the contribution of the 200-mb variability to the vertical shear variability. Therefore, with the ENI, the independent mechanism is still the equatorially confined upper- and lower-level zonal circulation dominated by the upper-level branch.

Vorticity fields from the covariances of the partials for the upper and lower levels discussed above (also not shown) demonstrate little change from the fields discussed in the previous section except in the relationship between the SI and the 200-mb-level winds with the variability explained by the ENI removed, where the area of anticyclonic vorticity is virtually eliminated. These results suggest that, with the influence of the SI and the ENI separated from each other, the role of vorticity in explaining some of the relationship between the SI and MH activity is reduced, at least at the 200-mb level, whereas its role in the association between the ENI and MH activity is maintained.

The partial regressions discussed above clarify the independent physical mechanisms that result in the anomalies of vertical shear that are associated with fluctuations in the ENI and the SI. The scalar covariance fields, based on partials between the ENI, the SI, and $|V_z|$, are given in Fig. 12. Comparison between $C(\mathrm{ENI}, |V_z||\mathrm{SI})$ (Fig. 12a) and $C(\mathrm{ENI}, |V_z|)$ (not shown) indicates that the effect of removing SI variability is to reduce the overall magnitude of the covariance in most of the region south of 25°N, especially near 10°N. Comparison between $C(\mathrm{SI}, |V_z||\mathrm{ENI})$ (Fig. 12b) and $C(\mathrm{SI}, |V_z|)$ (not shown) indicates that the effect of removing ENI variability also reduces the overall magnitude of the covariance in most of the region south of 20°N, but this time, especially south of ~10°N, the lower limit of the main development region. In addition, the overall areas of statistically significant correlations in the main development region shown in Figs. 12a,b are reduced from the statistically significant areas in that region for $r(\mathrm{ENI}, |V_z|)$ (see Fig. 7) and $r(\mathrm{SI}, |V_z|)$ (Fig. 9), respectively.

To summarize the comparison of the independent associations between the ENI and $|V_z|$, and the SI and $|V_z|$, differences between the magnitudes of the covariances shown in Figs. 12a,b are presented in Fig. 12c. Areas of positive differences indicate where the anomalies associated with the SI are greater than the anomalies associated with the ENI. The map clearly shows that the anomalies associated with the SI dominate the ENI influence in virtually the entire main development region. Areas of negative differences, indicating anomalies associated with the ENI dominating the SI influence, occupy the regions in the Atlantic basin from the equator to ~10°N and from ~20° to 30°N. Thus, even though $C(\mathrm{ENI}, |V_z||\mathrm{SI})$ has a larger and stronger statistically significant region than $C(\mathrm{SI}, |V_z||\mathrm{ENI})$, the strongest values are south of the main

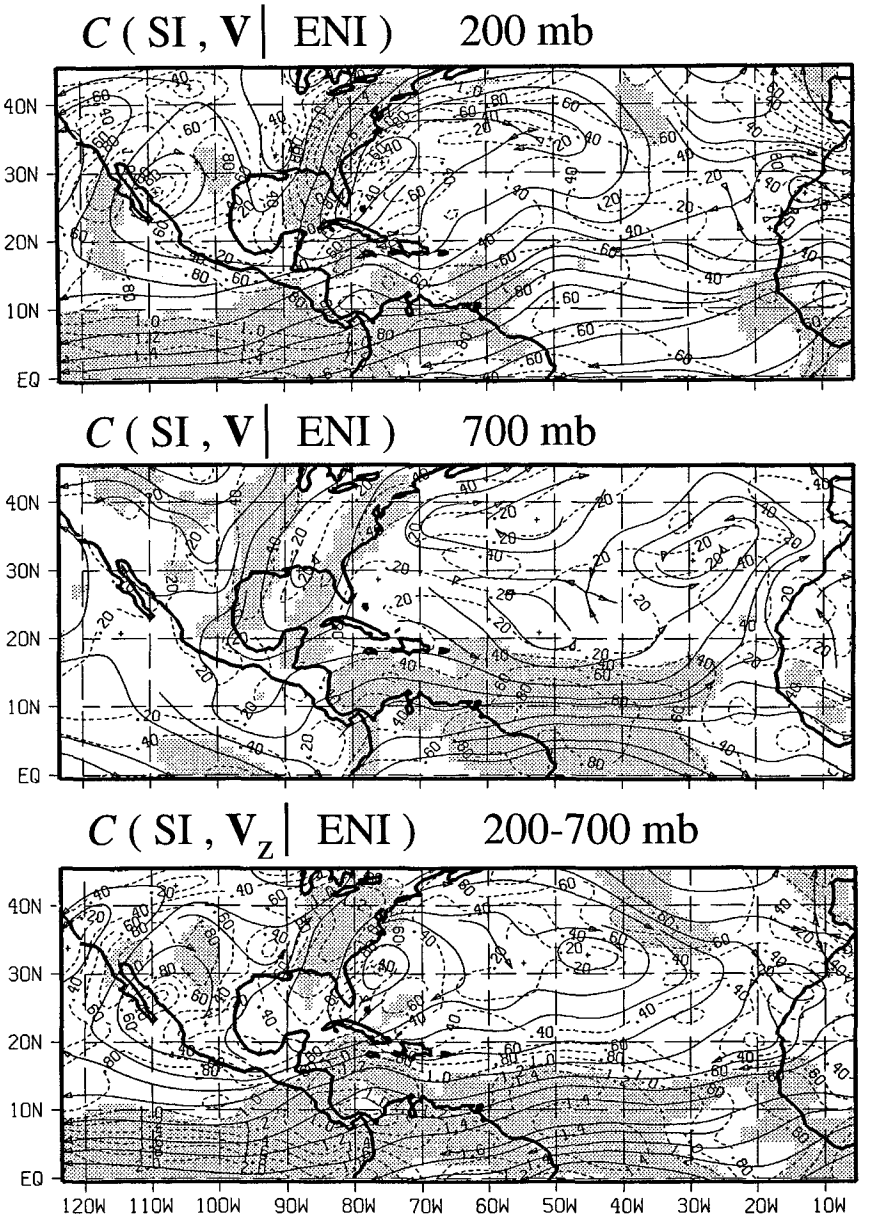


FIG. 11. Same as Fig. 8 but for the relationship between the SI and winds, as well as $V_z$, with the variability explained by the ENI removed. Isotach interval is 0.2 m $s^{-1}$.

development region. Therefore, the probable reason for the minimal independent contribution of contemporaneous ENI fluctuations to MH activity, as represented by the small value of $r$(MH, ENI|SI), is that the fluctuations in the magnitude of vertical shear in the main development region are primarily associated with fluctuations in the SI. Note that these results do not directly involve MHs and, therefore, can probably be generalized to include the other measures of Atlantic tropical cyclone activity.

### *b. Separating influences of the ENI and the SI from vertical shear*

The results presented in sections 3 and 4a strongly suggest that one of the physical mechanisms causing the relationships between the MHI and the ENI and between the MHI and the SI is the interannual variability in vertical shear over the main development region associated with ENI and SI fluctuations. The next step is to examine whether or not the ENI and the SI

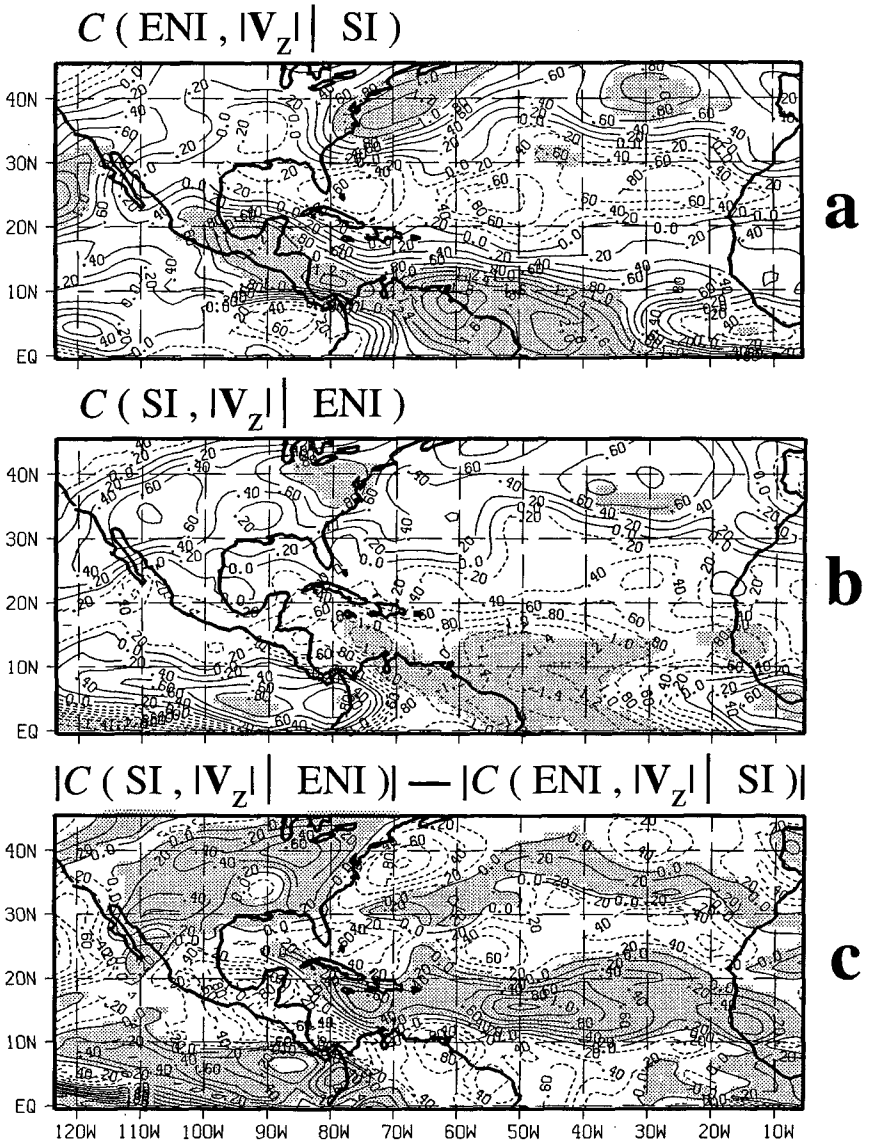


FIG. 12. Covariances for the relationships between (a) the ENI and $|V_z|$ with the variability explained by the SI removed and (b) the SI and $|V_z|$ with the variability explained by the ENI removed. Regions where the linear correlations for the relationship are significant at the 95% significance level are shaded. The difference between the absolute magnitudes, |(b)| − |(a)|, is given in (c). Isotach interval is 0.2 m $s^{-1}$.

contain additional information about the MHI *apart from* that due to their association with the fluctuations in vertical shear. Figure 13 shows the multiple partial correlation, $r^2$(MHI; ENI, SI| $|V_z|$), which is the fractional variance of MHI explained by ENI and SI after the variance explained by $|V_z|$ is removed. The minima along 10°N between 40° and 70°W indicate that, given information about $|V_z|$ in that portion of the basin, the SI and the ENI explain only ~25% of the remaining variance of the MHI. In addition, there is a minimum near 15°N on the West African coast. These results indicate that the SI and the ENI contain a small, but not negligible, amount of information on MH activity beyond that contained in the winds, particularly reflected in $|V_z|$ in the region where some of the waves develop into depressions (see Fig. 2) and in the region where the easterly waves move off the coast. Virtually all of the residual information is, in fact, due to the SI; the map of $r^2$(MHI; ENI| $|V_z|$) (not shown) indicates that the ENI provides essentially no additional information about the MHI beyond that provided by knowledge of $|V_z|$ in the southern portion of the basin. Figure 13

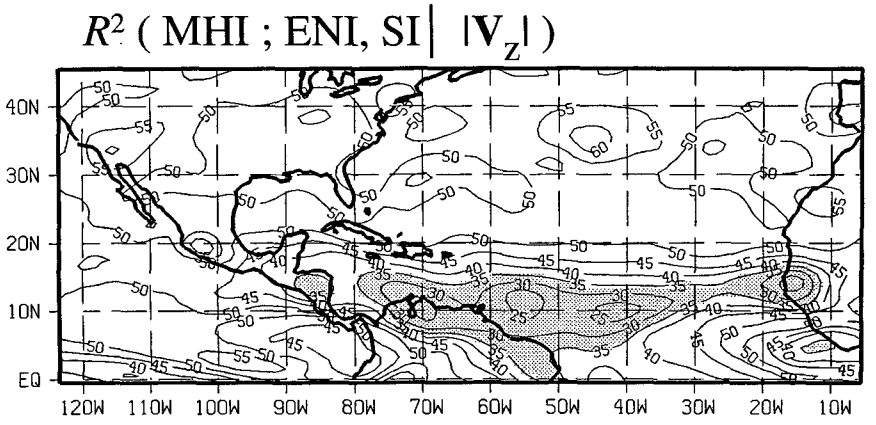


FIG. 13. Square of the multiple linear correlation coefficients [i.e., reduction of variance (ROV)] between the MHI and both the ENI and the SI, with the variability explained by $|V_z|$ removed. Magnitudes are multiplied by 100; contour interval is 0.05. Regions where ROV is less than 0.35 are shaded.

demonstrates that, although $|V_z|$ explains a substantial part of the association between the SI and the MHI, other mechanisms, such as variations in the strength of the easterly waves, may also contribute to the association, as suggested by Landsea and Gray (1992).

One final issue is whether there is any information contained in the relationship between the MHI and $|V_z|$ that cannot be attributed to their relationship with the ENI and the SI. Figure 14 shows the partial correlation between the MHI and $|V_z|$ with the variability explained by ENI and SI removed. The area of significant correlations between the MHI and $|V_z|$ is substantially reduced in the partial correlation, $r$(MHI, $|V_z|$ |ENI, SI), from the simple correlation in Fig. 6. There still remains a small area of significant correlations, however, in the development region between ~10° and 15°N and 55° and 70°W in the eastern Caribbean. These results indicate that there are interannual fluctuations in $|V_z|$ not associated with the ENI and the SI that still have significant associations with MH activity.

As illustrated in Figs. 15a,b, which show the covariances $C$(MHI, $V_z$) and $C$(MHI, $V_z$|ENI, SI), respectively, the removal of the variability associated with the ENI and the SI effectively eliminates the equatorially confined zonal circulation south of 10°N so evident in $C$(MHI, $V_z$). The remaining fluctuations in $V_z$ and $|V_z|$ that affect MH activity (Figs. 14 and 15b) appear to be associated with a cross-equatorial flow occupying the area between the equator and 20°N, and which extends across the entire analysis domain. This flow, for which the main contribution is at the 200-mb level (not shown), produces the easterly anomalies in the development region associated with the residual area of significant correlations in Fig. 14.

## 5. Summary and discussion

Correlations using 25 years of wind data for the 200- and 700-mb levels have elucidated the primary physical mechanisms responsible for the contemporaneous relationships shown in earlier studies between the number of August–October major hurricanes in the North Atlantic basin, an index of western Sahelian monsoon rainfall amounts, and an equatorial eastern Pacific SST index of El Niño. Partial correlations have been used to isolate some of the relationships associated with the various indices. The data used in the present study are for ASO, the most active months of the Atlantic hurricane season, with the exception of the rainfall data, which are for June–September (see section 2). Some of the results in this study have established relationships between the rainfall, El Niño indices, and the winds that do not involve major hurricanes and, therefore, could be generalized to include other measures of Atlantic basin tropical cyclone activity.

The results consistently support the conclusion that the upper- and lower-level winds over the region in the basin between ~10° and 20°N, where most of the tropical cyclones that eventually reach major hurricane strength begin development, are critical determinants of the number of major hurricanes in each hurricane season. In particular, as shown in previous studies, interannual fluctuations in the upper- and lower-level winds that produce changes in the magnitude of vertical shear ($|V_z|$) in that region are one of the most important factors associated with changes in seasonal major hurricane activity. In the present study, changes in vertical shear have been related to changes in the western Sahelian rainfall and eastern Pacific SSTs. As noted in section 3c, the shear patterns appear to be established several months before the time when MHs form and, therefore, are not solely due to the developing storms themselves.

Most of the correlation between the Sahelian rainfall fluctuations, as well as eastern Pacific SST fluctuations, and the interannual variations in the number of major hurricanes appears to be the result of an equatorially

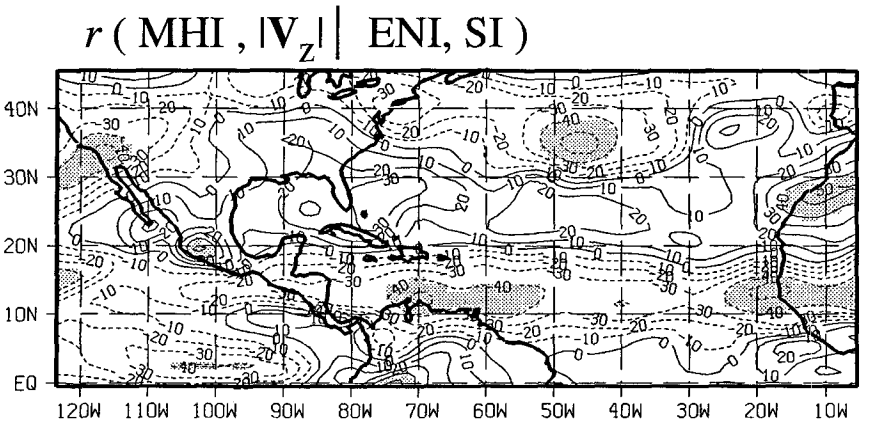


FIG. 14. Same as Fig. 6 but for the correlation between the MHI and $|V_z|$ with the variability explained by both the ENI and the SI removed.

confined zonal circulation that contributes to changes in $|V_z|$ over the main development region (between ~10° and 20°N). In years with positive (wet) rainfall anomalies, the circulation anomalies strongly resemble the circulation to the west of the ascending branch of a Walker cell, which might be forced by enhanced convection over western Africa and the adjacent water. In years with positive (warm) SST anomalies in the eastern Pacific, the circulation anomalies are of the opposite sense, such as might be forced by enhanced convection over the central and eastern Pacific during an El Niño event. Additional analysis would be required, however, to establish the mechanism that creates the circulation anomalies.

When El Niño–related effects are removed from the Sahel rainfall–associated circulations, the magnitude of the contributions from the upper- and lower-level branches are comparable (Fig. 11). The strongest correlations, however, appear to be from the lower-level branch. This result shows the importance of the low-level contribution to the relationship between the SI and $V_z$ in the main development region.

For the dataset used in the present study, the variance in the number of major hurricanes explained by the rainfall parameter is almost three times greater than that explained by the eastern Pacific SST parameter. It appears that the principal reason for the dominance of the rainfall-related effect is that the changes in $|V_z|$ in the main development region are more influenced by associations with changes in rainfall than by changes related to eastern Pacific SST anomalies (Fig. 12c). Although the SST-related $|V_z|$ anomalies in the Tropics are actually stronger than the anomalies associated with rainfall, the SST-related maxima are south of the main development region. Since a larger percentage of major hurricanes have their origins from easterly waves than weaker hurricanes or tropical storms, and since for the time period of this study almost 90% of those waves began to intensify in the main development region, it is not surprising that, of the various measures of Atlantic basin tropical cyclone activity, major hurricane activity shows the strongest correlation with the rainfall parameter (Landsea and Gray 1992).

The results indicate that not all of the relationship between rainfall and major hurricane fluctuations in the present study is due to changes in $|V_z|$ (see Fig. 13). Landsea and Gray (1992) suggest other mechanisms for the relationship, such as interannual variability in the character of the easterly waves themselves. If the waves are weaker during drier years, this could also lead to fewer waves developing into major hurricanes. The differences in wave characteristics between wet and dry years have not yet been established. Part of the relationship between rainfall and tropical cyclone activity and between the SSTs and tropical cyclone activity might also be due to associated vorticity changes in the upper or lower troposphere. Complementary changes in the vorticity accompany most of the results that were presented. Since removal of the variability explained by SST anomalies reduces the rainfall-related vorticity at 200 mb (section 4a), however, the role of vorticity in influencing major hurricane activity may be minimal. Other environmental factors associated with Sahel rainfall fluctuations influencing seasonal major hurricane activity, such as *local* SST fluctuations in the Atlantic basin, may also explain part of the relationship (Shapiro 1982b). These relationships are a topic of further investigation to be presented elsewhere.

In addition, it was shown that most of the variability in $|V_z|$ related to major hurricane activity is associated with the rainfall and SST fluctuations. A residual area of statistically significant correlations between major hurricanes and $|V_z|$ after rainfall and SST effects were removed (Fig. 14) suggests, however, the existence of additional factors that may be associated with the $|V_z|$ fluctuations in the main development region.

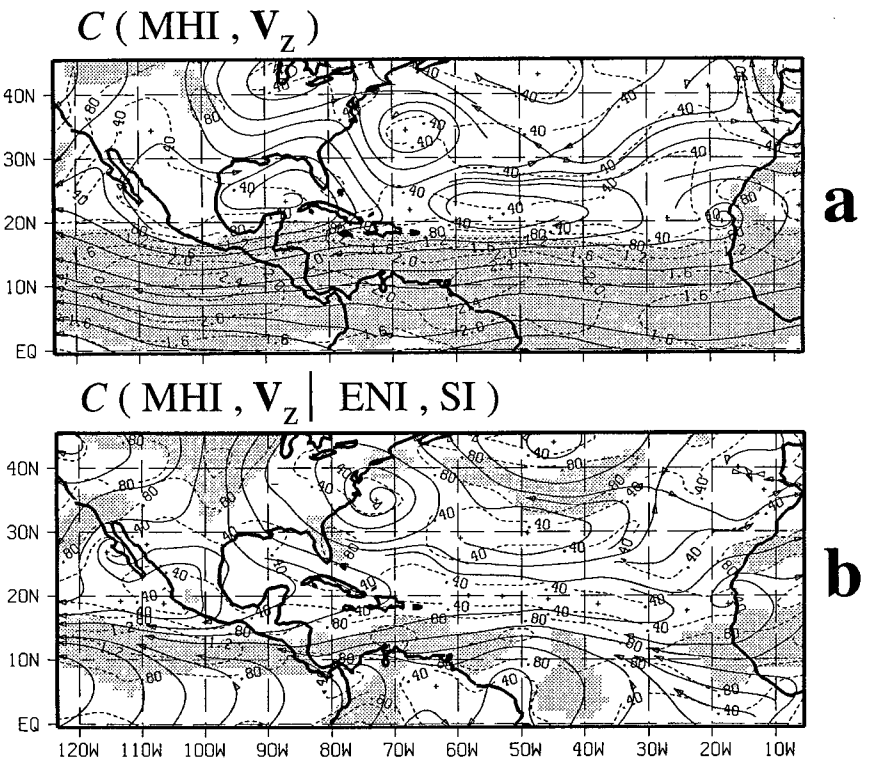


FIG. 15. Same as Fig. 8 but for the relationships between (a) the MHI and $V_z$ and (b) the MHI and $V_z$ with the variability explained by both the ENI and the SI removed. Isotach interval is 0.4 m $s^{-1}$.

The correlation patterns for major hurricanes with $|V_z|$ (Fig. 6) and both rainfall and SST associations with $|V_z|$ (Figs. 7, 9, 12a, and 12b) display a region to the north of the main development region where the sign of the correlations are reversed from the sign in the development region. The eastern Pacific SST-related changes in $|V_z|$ dominate over rainfall-related changes in this northern region between ~20° and 30°N (Fig. 12c). Although the correlations in most of this northern region are not statistically significant, the spatial coherence of these correlation patterns invites some speculation about their physical importance. The results suggest that, for most of the region to the north of the main development region, the fluctuations in $|V_z|$ are unrelated to or even out of phase with $|V_z|$ fluctuations in the development region. The lack of statistical significance for most of the fluctuations in the northern region is an expected consequence of the equatorially confined nature of the zonal circulations that are the primary physical mechanism for both the SST- and rainfall-related fluctuations of $|V_z|$. The possibly out-of-phase nature of the relationship between the north and south regions could be due to a change in the strength of the mid-Atlantic tropical upper-tropospheric trough, as suggested by Gray (1994) or, as suggested by Shapiro (1987), an association with the Pacific/North American pattern. The relationship suggests a possible physical explanation for the conclusions drawn by Gray and Landsea (1992) and Landsea et al. (1992), that in general major hurricane activity affecting the Gulf Coast seems unrelated to activity elsewhere in the Atlantic basin, as well as for the evidence presented by Gray (1994) for an inverse relationship between hurricanes in the Atlantic forming to the north and south of 25°N (see section 1). During years with increased $|V_z|$ in the main development region, $|V_z|$ could be slightly decreased in the ~20°–30°N band to the north. Thus, the northern region will remain close to the climatological vertical shear (see Fig. 3), which for most of that region is already close to or less than the suggested Hebert (1978) 5 m $s^{-1}$ threshold for development. Therefore, years of below-normal rainfall (drought) or above-average SSTs (El Niño conditions), which would yield unfavorable conditions for development in the main development region, would still allow for major hurricane development to the north from easterly waves or tropical cyclones that "survive" the journey through the unfavorable conditions to the south as well as from midlatitude or subtropical systems. Since the correlations between the El Niño index and $|V_z|$ (Fig. 7) and between the rainfall index and $|V_z|$ (Fig. 9) do not explicitly include information about major hurricane activity, the results should also apply to other hurri-

canes and tropical storms. Fewer of these other systems should be able to form from easterly waves in the main development region during the warmer (SST) and/or drier (rainfall) years but could still develop to the north during those years.

Caution must be exercised when applying relationships based on the correlations in the present study. Although statistically significant relationships were found, 25 years is still a relatively short period, especially given the evidence for multidecadal-type changes in the western African rainfall and major hurricane activity (e.g., Landsea 1991) and the character of El Niño events (Wang 1995). All of the 25 years fall within the long-term drought that has been afflicting the western Sahel. As discussed in section 2 and in Landsea and Gray (1992), the correlation between the rainfall and major hurricane activity shows great stability and is about the same between the wet and dry periods. It is quite possible, however, that the physical mechanisms based on the correlations discussed in the present study would be altered somewhat if data during only the wetter decades (i.e., 1949–67) or a longer period encompassing both wet and dry decades were used. In comparing the 25 years of data used in the present study to data extending back to 1949, fluctuations in the El Niño index were reasonably well sampled—in spite of the decadal-scale changes in the character of El Niño events, the full range was represented in the shorter record, and the standard deviation is virtually the same as for the longer (44-yr) record. The fluctuations in rainfall, however, are not well represented; the range and standard deviation of the shorter record are less than 70% of those for the longer record. This implies that the fluctuations in $|V_z|$ related to variability in the El Niño index were probably well represented in the present study. The magnitude of the $|V_z|$ fluctuations associated with rainfall variability, on the other hand, might have been underestimated. The potential increase of the rainfall-associated $|V_z|$ fluctuations would probably accentuate the results in the present study that have already indicated that the rainfall-associated $|V_z|$ fluctuations tend to be the main factor affecting intensification in the main development region. The accessibility in the near future of reanalyses of available atmospheric data by the NCEP (Kalnay and Jenne 1991) back to the mid-1950s holds the promise of substantially increasing the usable length of record.

Recent studies have identified two types of El Niño events associated with different phases of atmospheric coupling likely controlling the teleconnection between the equatorial eastern Pacific SST anomalies and Sahel monsoonal rainfall amounts (e.g., Ward et al. 1994). The probably nonhomogeneous physical mechanisms for the teleconnections contained in the data for 1968–92 would suggest a stratification of the years to better resolve the different mechanisms. The grouping of the 25 years of data together in the present study gives an overall, possibly overly simplistic, picture of the relationships. Progress is underway on the application of various stratification methodologies to the present problem.

El Niño–associated equatorial eastern Pacific SST anomalies are typically largest in the spring, out of phase with the summer Atlantic hurricane season. Other investigators have found a delayed atmospheric response to eastern Pacific SST anomalies. In particular, Reid et al. (1989) found a maximum correlation between the SST variability and tropospheric temperatures at Curacao approximately 3.5 months later. Research has begun that includes a closer examination of lag (predictive) relationships between eastern Pacific SSTs and both the ASO circulation anomalies and tropical cyclone activity. In addition, the impact of the eastern Pacific SST anomalies on the Atlantic circulation will be examined, as related to the temporal and spatial evolution of El Niño events. Particular attention will be given to those features, such as vertical shear, that impact the character of the hurricane season.

*Acknowledgments.* The authors wish to thank Abraham Oort and Vern Kousky of NOAA for providing the GFDL SST analyses and CPC El Niño index data, respectively. Robert Kohler provided invaluable programming and data processing assistance, and Bret Christoe assisted in both data processing and analysis. Special appreciation is extended to Joseph Griffin and Christian Labbé for computational support. We also are grateful to Lixion Avila, David Enfield, Charlie Neumann, and Richard Pasch for helpful discussions. James Franklin and Mark DeMaria provided useful comments on an earlier version of the paper. In addition, we wish to thank William Gray, Neil Ward, Christopher Landsea, and an anonymous reviewer for their constructive suggestions. This research was supported in part by the Equatorial Pacific Ocean Climate Studies Program of NOAA.

## REFERENCES

Arkin, P. A., 1982: The relationship between interannual variability in the 200 mb tropical wind field and the Southern Oscillation. *Mon. Wea. Rev.*, **110,** 1393–1404.

Dey, C. H., 1989: The evolution of objective analysis methodology at the National Meteorological Center. *Wea. Forecasting,* **4,** 297–312.

Folland, C. K., T. N. Palmer, and D. E. Parker, 1986: Sahelian rainfall and worldwide sea temperatures 1901–1985. *Nature,* **320,** 602–607.

——, J. A. Owen, M. N. Ward, and A. W. Colman, 1991: Prediction of seasonal rainfall in the Sahel region using empirical and dynamical methods. *J. Forecasting,* **10,** 21–56.

Frank, N. L., 1975: Atlantic tropical systems of 1974. *Mon. Wea. Rev.*, **103,** 294–300.

Gray, W., 1968: Global view of the origin of tropical disturbances and storms. *Mon. Wea. Rev.*, **96,** 669–700.

——, 1984a: Atlantic seasonal hurricane frequency. Part I: El Niño and 30 mb quasi-biennial oscillation influences. *Mon. Wea. Rev.*, **112,** 1649–1668.

——, 1984b: Atlantic seasonal hurricane frequency. Part II: Forecasting its variability. *Mon. Wea. Rev.*, **112,** 1669–1683.

——, 1990: Strong association between West African rainfall and U.S. landfall of intense hurricanes. *Science,* **249,** 1251–1256.

——, 1994: Early August updated forecast of Atlantic seasonal hurricane activity for 1994. 24 pp. [Available from Department of Atmospheric Science, Colorado State University, Fort Collins, CO 80523.]

——, and C. W. Landsea, 1992: African rainfall as a precursor of hurricane-related destruction on the U.S. East Coast. *Bull. Amer. Meteor. Soc.,* **73,** 1352–1364.

——, ——, P. W. Mielke Jr., and K. J. Berry, 1993: Predicting Atlantic basin seasonal tropical cyclone activity by 1 August. *Wea. Forecasting,* **8,** 73–86.

——, ——, ——, and ——, 1994: Predicting Atlantic basin seasonal tropical cyclone activity by 1 June. *Wea. Forecasting,* **9,** 103–115.

Hebert, P. J., 1978: Intensification criteria for tropical depressions of the western North Atlantic. *Mon. Wea. Rev.,* **106,** 831–840.

——, and G. Taylor, 1979: Everything you always wanted to know about hurricanes—Part II. *Weatherwise,* **32,** 100–107.

——, J. D. Jarrell, and M. Mayfield, 1993: The deadliest, costliest and most intense United States hurricanes of this century (and other frequently requested hurricane facts). NOAA Tech. Memo. NWS NHC 31, 41 pp. [Available from Tropical Prediction Center, 11691 S.W. 17th St., Miami, FL 33165-2149.]

Hess, J. C., 1994: Improved seasonal predictions of hurricane activity for the Atlantic basin. M.S. thesis, Department of Meteorology, The Florida State University, Tallahassee, FL, 64 pp. [Appendix available on-line at ftp://metlab1.met.fsu.edu/pub/elsner/Appendix.]

Jarvinen, B. R., C. J. Neumann, and M. A. S. Davis, 1984: A tropical cyclone data tape for the North Atlantic basin, 1886–1983: Contents, limitations, and uses. NOAA Tech. Memo. NWS NHC 22, 21 pp. [Available from Tropical Prediction Center, 11691 S.W. 17th St., Miami, FL 33165-2149.]

Kalnay, E., and R. Jenne, 1991: Summary of the NMC/NCAR reanalysis workshop of April 1991. *Bull. Amer. Meteor. Soc.,* **72,** 1897–1904.

Kleinbaum, D., and L. Kupper, 1978: *Applied Regression Analysis and Other Multivariable Methods.* Duxbury Press, Wadsworth Publishing, 556 pp.

Kurihara, Y., and R. E. Tuleya, 1981: A numerical simulation study on the genesis of a tropical storm. *Mon. Wea. Rev.,* **109,** 1629–1653.

Lamb, P. J., 1982: Persistence of Subsaharan drought. *Nature,* **299,** 46–48.

Landsea, C. W., 1991: West African monsoonal rainfall and intense hurricane associations. Dept. of Atmos. Sci. Paper 484, Colorado State University, Fort Collins, CO, 272 pp.

——, 1993: The climatology of intense (or major) Atlantic hurricanes. *Mon. Wea. Rev.,* **121,** 1703–1713.

——, and W. M. Gray, 1992: The strong association between western Sahelian monsoon rainfall and intense Atlantic hurricanes. *J. Climate,* **5,** 435–453.

——, ——, P. W. Mielke Jr., and K. J. Berry, 1992: Long-term variations of western Sahelian monsoon rainfall and intense U.S. landfalling hurricanes. *J. Climate,* **5,** 1528–1534.

——, ——, ——, and ——, 1993: Predictability of seasonal Sahelian rainfall by 1 December of the previous year and 1 June of the current year. Preprints, *20th Conf. on Hurricane and Tropical Meteorology,* San Antonio, TX, Amer. Meteor. Soc., 473–476.

Mayfield, M., L. Avila, and E. N. Rappaport, 1994: Atlantic hurricane season of 1992. *Mon. Wea. Rev.,* **122,** 517–538.

Neumann, C. J., B. R. Jarvinen, C. J. McAdie, and J. D. Elms, 1993: *Tropical Cyclones of the North Atlantic Ocean, 1871–1992.* National Climatic Center, 193 pp.

Newell, R. E., and J. W. Kidson, 1984: African mean wind changes between Sahelian wet and dry periods. *J. Climatol.,* **4,** 27–33.

Oort, A. H., Y. H. Pan, R. W. Reynolds, and C. F. Ropelewski, 1987: Historical trends in the surface temperature over the oceans based on the COADS. *Climate Dyn.,* **2,** 29–38.

Pasch, R. J., and L. A. Avila, 1992: Atlantic hurricane season of 1991. *Mon. Wea. Rev.,* **120,** 2671–2687.

——, and ——, 1994: Atlantic tropical systems of 1992. *Mon. Wea. Rev.,* **122,** 539–548.

Quinn, W. H., and V. T. Neal, 1987: El Niño occurrences over the past four and a half centuries. *J. Geophys. Res.,* **92,** 14 449–14 461.

——, D. O. Zopf, K. S. Short, and R. T. Kuo Yang, 1978: Historical trends and statistics of the Southern Oscillation, El Niño, and Indonesian droughts. *Fish. Bull.,* **76,** 663–678.

Reed, R. J., D. C. Norquist, and E. E. Recker, 1977: The structure and properties of African wave disturbances as observed during Phase III of GATE. *Mon. Wea. Rev.,* **105,** 317–333.

Reid, G. C., K. S. Gage, and J. R. McAfee, 1989: The thermal response of the tropical atmosphere to variations in equatorial Pacific sea surface temperature. *J. Geophys. Res.,* **94,** 14 705–14 716.

Shapiro, L., 1982a: Hurricane climatic fluctuations. Part I: Patterns and cycles. *Mon. Wea. Rev.,* **110,** 1007–1013.

——, 1982b: Hurricane climatic fluctuations. Part II: Relation to large-scale circulation. *Mon. Wea. Rev.,* **110,** 1014–1023.

——, 1984: Sampling errors in statistical models of tropical cyclone motion: A comparison of predictor screening and EOF techniques. *Mon. Wea. Rev.,* **112,** 1378–1388.

——, 1987: Month-to-month variability of the Atlantic tropical circulation and its relationship to tropical storm formation. *Mon. Wea. Rev.,* **115,** 2598–2614.

Siegel, S., 1956: *Nonparametric Statistics.* McGraw-Hill, 312 pp.

Simpson, R. H., 1974: The hurricane disaster potential scale. *Weatherwise,* **27,** 169–186.

Wang, B., 1995: Interdecadal changes in El Niño onset in the last four decades. *J. Climate,* **8,** 267–285.

Wang, X., 1993: The global climate for March–May 1992: Mature phase warm episode continues in the tropical Pacific. *J. Climate,* **6,** 2465–2485.

Ward, M. N., K. Maskell, C. K. Folland, D. P. Rowell, and R. Washington, 1994: A tropic-wide oscillation of boreal summer rainfall and patterns of sea-surface temperature. Climate Res. Tech. Note 48, 16 pp. [Available from Hadley Centre for Climate Prediction and Research, Meteorological Office, London Road, Bracknell, Berkshire RG12 2SY, United Kingdom.]